

# Activity-based Sensing of Ascorbate using Copper-Mediated Oxidative Bond Cleavage

Zuo Hang Yu,<sup>[a]</sup> Christopher J. Reinhardt,<sup>[b]</sup> Thomas Hin-Fung Wong,<sup>[a]</sup> Ka Yan Tong,<sup>[a]</sup> Jefferson Chan,<sup>[b]</sup> and Ho Yu Au-Yeung<sup>\*[a]</sup>

[a] Z. H. Yu, T. H.-F. Wong and Dr. H. Y. Au-Yeung  
Department of Chemistry  
The University of Hong Kong  
Pokfulam Road, Hong Kong, P. R. China  
E-mail: hoyuay@hku.hk

[b] C. J. Reinhardt and Prof. J. Chan  
Department of Chemistry  
University of Illinois at Urbana Champaign  
Urbana, Illinois 61801, United States

Supporting information for this article is given via a link at the end of the document.

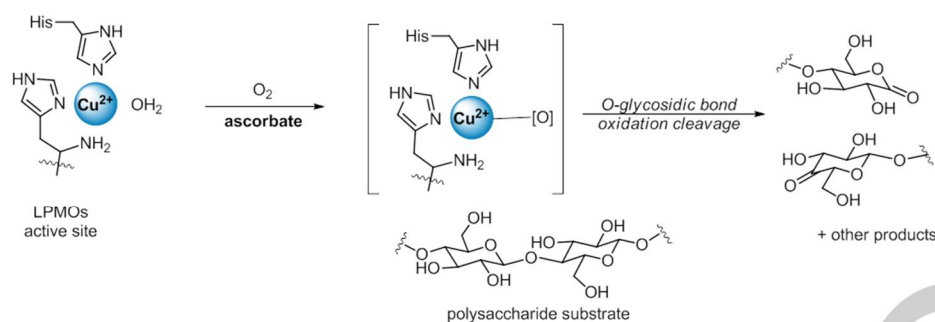
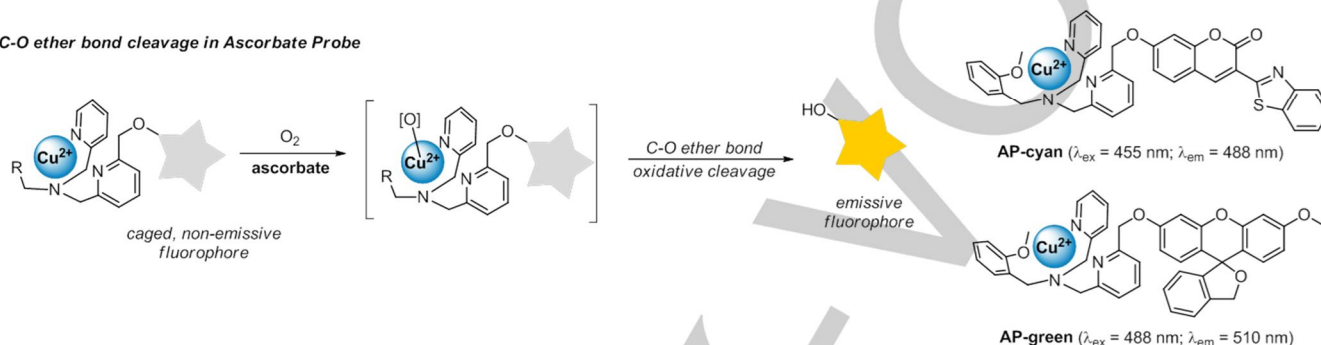
**Abstract:** Ascorbate is an important biological reductant and enzyme cofactor. While direct detection via ascorbate-mediated reduction is possible, this approach suffers from poor selectivity due to the wide range of cellular reducing agents. To overcome this limitation, we leverage ascorbate's reduction potential to mediate a copper-mediated oxidative bond cleavage of ether-caged fluorophores. The copper(II) complexes supported by a {bis(2-pyridylmethyl)benzylamine} or a {bis(2-pyridylmethyl)}(2-methoxybenzyl)amine ligand were identified as an ascorbate responsive unit and their reaction with ascorbate yields a copper-based oxidant that enables rapid benzylic oxidation and the release of the ether-caged dye (coumarin or fluorescein). The copper-mediated bond cleavage is specific to ascorbate and the trigger can be readily derivatized for tuning photophysical properties. The probes were successfully applied for the fluorometric detection of ascorbate in commercial food samples, human plasma and serum, and within live cells using confocal microscopy and flow cytometry.

## Introduction

Ascorbate (vitamin C) is biosynthesized in plants and animals from a monosaccharide precursor (e.g., glucose or galactose). Interestingly, some primates, including humans, have lost the ability to make ascorbate. For this reason ascorbate is an essential nutrient for human and has been consumed as a non-prescribed supplement.<sup>[1]</sup> Under physiological conditions, ascorbate exists mainly as a monoanion.<sup>[2]</sup> One-electron oxidation of ascorbate generates ascorbyl radical which can be further oxidized to dehydroascorbate (DHA). The biochemical function of ascorbate is often related to its interconversion between redox forms.<sup>[3]</sup> Along with other cellular redox cycles, ascorbate regulates cellular oxidative stress and redox signaling which are both implicated in aging and diseases.<sup>[4]</sup> Ascorbate also serves as an enzyme cofactor for collagen<sup>[5]</sup> and carnitine biosynthesis,<sup>[6]</sup> the amidation of peptide hormones,<sup>[7]</sup> and the hydroxylation of dopamine to noradrenaline.<sup>[8]</sup> For its diverse occurrence and importance, there are different debates and controversies related to the health benefits and roles of

ascorbate in disease treatments and therapies.<sup>[9]</sup> As a result, quick, selective and sensitive ascorbate sensing methods are of high importance for both clinical applications and fundamental physiological studies.

Selective detection of ascorbate is challenging in complex biological matrices (e.g., live cells). Conventional HPLC,<sup>[10]</sup> electrochemical methods<sup>[11]</sup> and plate reader assays<sup>[12]</sup> only provide the total ascorbate content (all redox states). Moreover, these methods require sample pretreatment, extraction and derivatization with limited spatiotemporal information. Luminescent techniques, on the other hand, are non-destructive, sensitive and operationally simple.<sup>[13]</sup> Additionally, appropriate probe and experiment design can yield information regarding cellular distribution, redox state and interplay with other cellular components. Unfortunately, there are only a limited number of ascorbate luminescent probes with live cell capabilities. The most common and straightforward strategy for designing ascorbate probes employs the direct reduction of a paramagnetic quencher (e.g. a TEMPO radical).<sup>[14]</sup> A key drawback to this approach is the wide redox potential window displayed by cellular oxidants and reductants that poses concerns regarding undesirable probe activation. Unfortunately, it is challenging to overcome these cross-reactivity problems when the responsive moiety is based on a promiscuous redox reaction. To address this, we turned our attention to lytic polysaccharide monooxygenases (LPMOs), a class of copper monooxygenases that can employ ascorbate as a cofactor for the oxidative cleavage of polysaccharides.<sup>[15]</sup> By mimicking the catalytic mechanism of the enzyme, it would be possible to couple ascorbate-mediated reduction of a copper complex to induce benzylic oxidation of an ether. Selective coupling of a reporter dye to the responsive element would enable a fluorescent response (Scheme 1). Herein, we report the development of a generalizable responsive element for the detection of ascorbate. The two fluorescent ascorbate probes, AP-cyan and AP-green, employ an ascorbate-induced, copper-mediated C-O ether bond cleavage that is similar to LPMOs. Both probes display good selectivity against a range of redox

*O*-glycosidic bond cleavage by LPMOs*C*-O ether bond cleavage in Ascorbate Probe

**Scheme 1.** LPMOs employ ascorbate as a cofactor for  $\text{O}_2$  activation and *O*-glycosidic bond oxidative cleavage of polysaccharide substrate (top). The LPMOs inspired design of fluorescent ascorbate probes featuring an ether bond cleavage for fluorophore uncaging (bottom).

active biomolecules and are applicable in various complex matrices, such as commercial food samples, human plasma, and serum using a plate reader assay, and also in live cells using confocal microscopy and flow cytometry.

## Results and Discussion

**Design of the Copper-based Ascorbate Probes.** LPMOs are a class of monooxygenase that can employ ascorbate as a cofactor for dioxygen activation at a mononuclear copper site. The resulting metal center is then poised for oxidation of the substrate (e.g., C-H hydroxylation or oxidative cleavage of glycosidic bonds). The active-site structure of LPMOs was recently characterized as a mononuclear copper coordinated by two histidine imidazoles and one peptidyl  $\text{NH}_2$  in a T-shaped geometry, named the "histidine brace".<sup>[15b,15f,15g,16]</sup> It has been established that ascorbate is an efficient electron donor required for dioxygen activation and substrate oxidation by LPMOs, and specificity for the electron source has also been demonstrated in different classes of LMPOs.<sup>[17]</sup> We reasoned that a functional mimic of LPMOs could be exploited as a new activity-based sensing platform for ascorbate detection (Scheme 1). Indeed, similar metal-based oxidation strategies have been successful for the development of selective metal and reactive oxygen species probes.<sup>[18,19]</sup> Collective evidence suggests that the metal reactivity towards the fluorophore's oxidative release is specific to the environment in both the first and secondary coordination sphere and the metal electronic structures. For this reason, the

ligand geometry and denticity, nature of coordination donors, and secondary groups can be systematically varied to tune the reactivity and selectivity of probes towards different target analytes.

Our design of a bond cleavage-based ascorbate probe consists of a fluorophore linked to an ascorbate-responsive unit. For example, **1-Cu** contains a {bis(2-pyridylmethyl)benzylamine coordinated Cu(II), designed as a synthetic analog of the "histidine brace" where it contains two  $sp^2$  and one  $sp^3$  nitrogen donor, is linked to a fluorescein in its non-emissive form. When the fluorescein is caged as an ether,  $\pi$ -conjugation of the xanthene moiety is disrupted and renders the compound weakly absorbing and weakly emissive. An ether bond cleavage and keto-enol tautomerization of the released phenol will restore the  $\pi$ -conjugation and the uncaged fluorescein will become emissive. Similar fluorescence off-on control by caging the phenol group of coumarin- and xanthene-based fluorophores as an ether has also been exploited for developing photocaged fluorescent dyes and probes for metal ions and reactive species.<sup>[18-20]</sup> It is worth noting that the present strategy is different from most other copper-based fluorescent probes because the fluorescence enhancement is not due to the removal of the paramagnetic  $\text{Cu}^{2+}$  quencher, but the specific chemical reactivity of ascorbate with the copper. This key difference provides the necessary ascorbate selectivity by preventing false positive via simple  $\text{Cu}^{2+}$  reduction, competitive ligand exchange or other non-bond cleavage-leading reactions.<sup>[21]</sup> On the other hand, because of the irreversible nature of the bond cleavage that drives the complexation equilibrium, the cleaved fluorophore can be accumulated to result in a fluorescent signal despite of any potential competitive copper binding by other molecules, which

further distinguishes the current design from other metal-based probes that produce a fluorescent response via a simple reversible binding with the target analyte.

Treatment of **1-Cu** with ascorbate resulted in a 114-fold fluorescence enhancement, showing a histidine brace mimic is indeed responsive to ascorbate. Next, the responsive element was modified to contain oxygen ligands to mimic the subset of LMPOs which contain an axial tyrosine coordination in addition to the histidine brace.<sup>[15]</sup> Consistent with previous reports,<sup>[18,19]</sup> the reactivity of the copper complex was sensitive to the coordination environment where **3-Cu** (with a {bis(2-pyridylmethyl)}(2-hydroxybenzyl)amine ligand) and **4-Cu** (with a (2-pyridylmethyl){bis(2-hydroxyethyl)}amine ligand) had no significant fluorescent response (Figures 1 and S1).<sup>[22]</sup> On the other hand, an increased fluorescence turn-on was observed for **2-Cu**, which contains an {bis(2-pyridylmethyl)}(2-methoxybenzyl)amine ligand. More detailed studies are necessary to elucidate the roles and effect of different oxygen donors on the ascorbate reactivity. To determine if the counter ion played an effect on the fluorescence enhancement, **1-Cu** was prepared from copper(II) chloride, perchlorate or tetrafluoroborate, where no effect was observed (Figure S2). Finally, the ascorbate reactivity of the copper(II) complex was evaluated when the green emitting fluorescein dye ( $\lambda_{em} = 510$  nm) was replaced with the cyan emitting 3-(benzothiazole-2-yl)-7-hydroxycoumarin dye ( $\lambda_{em} = 488$  nm) (**5-Cu** and **6-Cu**). The two coumarin-based compounds were found to be also responsive towards ascorbate with a strong fluorescence turn-on, confirming that this ascorbate activity-based sensing strategy is modular (Figure 1). All together, these experiments demonstrate that the bioinspired oxidation is an effective strategy for fluorescent ascorbate sensing. It is worth noting that the selective triggering of metal-based oxidative reactivity by neither the metal nor the oxidant is indirect and non-trivial, therefore further distinguishes the present ascorbate sensing from most other current designs of activity-based sensing featuring metal reactivity.

Compound	R <sub>1</sub>	R <sub>2</sub>	fluorescence turn-on (F <sub>f</sub> /F <sub>i</sub> )
<b>1-Cu</b>	2-py	Ph	114
<b>2-Cu</b> (AP-green)	2-py	C <sub>6</sub> H <sub>4</sub> (2-OMe)	153
<b>3-Cu</b>	2-py	C <sub>6</sub> H <sub>4</sub> (2-OH)	4
<b>4-Cu</b>	CH <sub>2</sub> OH	CH <sub>2</sub> OH	10
<b>5-Cu</b>	2-py	Ph	149
<b>6-Cu</b> (AP-cyan)	2-py	C <sub>6</sub> H <sub>4</sub> (2-OMe)	198
<b>7-Cu</b>	2-py	C <sub>6</sub> H <sub>4</sub> (2-OMe)	/

**Figure 1.** Structures of copper(II) complex-fluorophore conjugates and their fluorescent response towards 20 eq. ascorbate after a 30-min reaction.

**Ascorbate Reactivity and Selectivity.** The ascorbate selectivity of **1-Cu**, **2-Cu**, **5-Cu** and **6-Cu** were evaluated in more detail. Solutions of all the four complexes are weakly emissive in aqueous buffer (pH 7.4) but showed a rapid fluorescence turn-on upon treatment with ascorbate. For example, **2-Cu** showed a ca. 65-fold and 153-fold fluorescence turn-on after 2 min and 30

min incubation with ascorbate, respectively (Figure 2). In all cases, the ascorbate response is fast with ~90% of the maximum fluorescence enhancement obtained within 10.15 minutes under all the studied conditions. For comparison, some activity-based probes for metal sensing could have a reaction time as long as 1 to 2 hours.<sup>[18]</sup> Considering that the reaction rate will be dependent on the local concentrations of both the probe and ascorbate in different samples, a common 30-minute reaction time is adopted for the subsequent studies. In addition, all of the four compounds displayed good selectivity against a panel of biological and inorganic reducing agents including NADH, lipoic acid,  $\alpha$ -tocopherol (vitamin E), and uric acid. Incubation with other common cellular or food components, such as sugars, amino acids, other vitamins, and acids also resulted in no appreciable fluorescent response (Figures 2 and S3). Importantly, no fluorescence turn-on was observed when the probes were treated with DHA, demonstrating a good selectivity for the reduced form (ascorbate).

In addition to the tuning of the metal reactivity, varying the coordination ligand in the ascorbate-responsive unit will also give probes of different stability. For example, **5-Cu** and **6-Cu** differ significantly in their stability against copper(II) dissociation despite their similar ascorbate reactivity and selectivity. Liquid chromatography mass spectrometry (LCMS) showed complete copper(II) dissociation from **5-Cu** under the acidic chromatographic conditions. On the other hand, **6-Cu** elutes as an intact complex with only partial copper(II) dissociation (Figure S14). The higher stability of **6-Cu** can be attributed to the weakly coordinating methoxy group that chelates to the metal. Isothermal titration calorimetry experiment showed that binding of the {bis(2-pyridylmethyl)}(2-methoxybenzyl)amine ligand to Cu<sup>2+</sup> is strong with a measured  $K_d$  value of ~170 nM, suggesting ~90% of the probe remained as the copper(II) complex in a 10  $\mu$ M probe solution (Figure S51). This result highlights the fact that careful design of the coordination ligand can result in favorable properties beyond sensitivity and selectivity. Subsequent studies were therefore focused on **2-Cu** (AP-green) and **6-Cu** (AP-cyan). To further evaluate the suitability of AP-cyan and AP-green for fluorescent ascorbate detection in complex matrix, their fluorescence response towards ascorbate was also measured in the presence of other biological reducing agents. As shown in Figure S4, a strong fluorescence enhancement was observed when AP-cyan or AP-green was treated with 20 eq. of ascorbate in the presence of other biological redox agents such as NADH,  $\alpha$ -tocopherol, CoQ<sub>10</sub> and dopamine, despite of a slight reduction of the overall fluorescence turn-on. The fluorescence response can be interfered by a high concentration of GSH (2 mM), but a strong and statistically significant ascorbate-induced emission enhancement can still be observed for both AP-cyan (16-fold) and AP-green (10-fold), and these fluorescence turn-on are indeed comparable with other activity-based probes that have been demonstrated to be applicable in cells (Figure S5). The interference from GSH could probably due to a competitive copper(II) coordination and/or a short-circuiting of the electron transfer between ascorbate and the probe. It will therefore be important to carefully characterize the analytical performance of the probe in different samples.



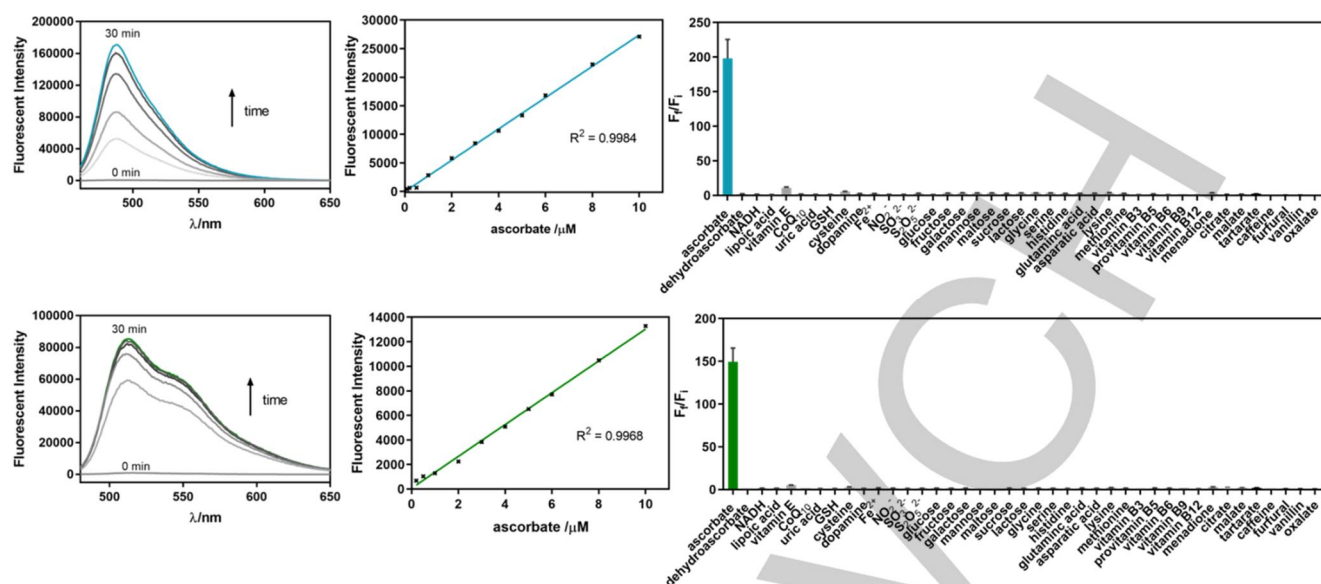


**Figure 2.** Fluorescent response of 5  $\mu$ M AP-green (top panel) and AP-cyan (bottom panel) in 50 mM HEPES at pH 7.4 at 298 K. Left: Time-dependent fluorescent response towards 20 eq. of ascorbate at 0, 4, 8, 12, 16, 20 and 30 min. Middle: dose-dependent fluorescent towards 1. 10  $\mu$ M ascorbate for 30 min. Right: selectivity against a panel of reducing agents, sugars, amino acids and vitamins (20 eq., except for GSH: 2 mM). AP-green and AP-cyan were excited at 470 nm and 450 nm, and the relative fluorescence intensity was measured at 510 nm and 488 nm respectively. Data is reported as mean  $\pm$  standard deviation ( $n = 3$ ).

#### Photostability, Aqueous Stability and Effect of pH.

Photostability of AP-cyan and AP-green was also evaluated. A 5  $\mu$ M solution of the probes was irradiated at 254 nm using a 6 W UV lamp for 30 minutes, and then the fluorescence response towards ascorbate was measured. The photo-irradiated probe solutions were found to give similar ascorbate-induced emission turn-on as from probe solutions that are prepared freshly, showing a good photostability of both AP-cyan and AP-green (Figure S6). In addition, similar fluorescence response was also observed from solutions of AP-cyan and AP-green that have been prepared and stored under ambient conditions for 3 days (Figure S7). Moreover, no significant difference in the ascorbate-induced fluorescence response of AP-green was observed when the measurement was conducted at pH 5 to pH 8, showing the probe can be applied in these biologically relevant pH values (Figure S8). Of note, a significant drop in the fluorescence intensity was observed from AP-cyan below pH 6, which is probably due to the presence of the non-emissive protonated form of 3-(benzothiazole-2-yl)-7-hydroxycoumarin ( $pK_a = 7.02$ ).<sup>[23]</sup> Nevertheless, the high modularity of the copper-based ascorbate trigger will allow the facile incorporation of fluorescent reporters to give probes of different photophysical, chemical and biological properties for use in specific experiments with different requirements.

**Mechanistic Studies.** The ascorbate-induced fluorescence turn-on was studied in more detail using AP-cyan. First, the proposed reaction products were confirmed via LCMS where ascorbate-treated AP-cyan yielded the uncaged coumarin ( $m/z = 296.2$ ; retention time = 4.7 min; yield = 44%) along with some other non-emissive oxidation products (Figure S16). This confirms that the observed fluorescence response was due to an ascorbate-induced ether bond cleavage. Next, molecular oxygen

was identified as the terminal oxidant, where no fluorescence turn-on was observed when AP-cyan was treated under anoxic conditions (Figure S9). Importantly, the fluorescence enhancement could be rescued upon re-introduction of air to the reaction mixture (Figure S10). In addition, the oxidative cleavage is dependent on the copper(II) center as treatment of the ligand-fluorophore conjugate **6** with ascorbate did not yield any fluorescent response (Figure S11). From these results, we hypothesize that the ether bond cleavage is due to a copper-based oxidant resulted from a reaction between the probe, ascorbate and molecular oxygen. To support this hypothesis, compound **6** was treated with reactive oxygen species (ROS) and no fluorescent response was observed (Figure S11). Moreover, incubating AP-cyan with different ROS gave no significant turn-on response (Figure S12). Indirect oxidation of the benzylic position was ruled out because no ROS were detected via different ROS probes under the same conditions (Figures S17 and S18). The presence of catalase or superoxide dismutase, which rapidly removes hydrogen peroxide and superoxide, also had no significant effect on the ascorbate-induced fluorescence turn-on of AP-cyan (Figure S13). These observations are consistent with the ether bond being cleaved by a copper-based oxidant rather than free ROS similar to a Fenton-like reaction.

While further mechanistic studies are warranted, it has been suggested that substrate oxidation by synthetic LMPOs mimics may involve a copper(II) hydroperoxo species. This intermediate has been characterized by a weak  $d-d$  transition at  $\sim 650$  nm and a strong LMCT in  $\sim 375$  nm.<sup>[24]</sup> The strong absorption of the coumarin and fluorescein fluorophores at  $\sim 350$ –470 nm may however preclude the characterization of any high energy absorption below 450 nm. Nevertheless, UV-Vis analysis of

ascorbate-treated AP-cyan also showed a weak absorption at 680 nm ( $\epsilon = 50 \text{ M}^{-1}\text{cm}^{-1}$ ) which is consistent with a copper(II) species in our system (Figure S23). A reversible redox couple at .212 mV (vs. NHE) was characterized by cyclic voltammetry for the model complex **7-Cu**,<sup>[25]</sup> indicating that an electron transfer from ascorbate to the copper(II) is thermodynamically feasible (Figure S26).<sup>[26]</sup> Under aerobic conditions, AP-cyan displayed a second order reaction kinetics (first order with respect to both ascorbate and AP-cyan). This suggests that electron transfer from ascorbate to the probe is possibly involved in the reaction. Indeed, HR-ESI-MS analysis of an immediate reaction mixture of AP-cyan and ascorbate also showed a new peak at  $m/z = 689.1269$ , which can be assigned as a one-electron reduced product of the probe (Figure S19). Although the detailed mechanism is likely complicated by the specific environment of the reacting ascorbate and copper in different samples,<sup>[27]</sup> the involvement of multiple redox-active species and the possibility of different electron transfer pathways (e.g., one versus two electron transfer, proton-coupled electron transfer),<sup>[28]</sup> it is clear that the bis(2-pyridylmethyl)amine coordinated copper(II) can effectively and selectively trigger the oxidative cleavage of the ether bond upon reaction with ascorbate.

**Ascorbate Detection in Drinks, Human Plasma and Serum Samples by AP-cyan.** Ascorbate is often added to consumer products (e.g., fruit juice, vitamin water, etc.) because of its antioxidant properties and nutritional properties. Moreover, ascorbate levels are clinically monitored to prevent scurvy or contaminations in the quantification of other bioanalytes.<sup>[29]</sup> To test the performance of the ascorbate probe in a plate reader assay, we chose to employ AP-cyan in real sample matrices. AP-cyan (limit of detection = 0.14 M by 3 method) was selected over AP-green (limit of detection = 0.48 M by 3 method) because of its superior sensitivity. AP-cyan was first tested in two commercial drink samples. As shown in Table 1, the measured ascorbate concentrations matched well with the values provided on the nutrition labels.<sup>[30]</sup> The probe was then applied in human plasma and serum samples. Under both conditions, the measured ascorbate concentrations were consistent with reported physiological concentrations.<sup>[31]</sup> The good recovery upon spiking with known concentrations of ascorbate indicate that the fluorescent measurement do not experience significant matrix effects. Together, these results indicate that AP-cyan can be used for a fast, sensitive, selective and high throughput measurement of ascorbate concentrations in real samples. Yet, with the very different compositions in different samples, especially the presence of competitive copper binders and redox agents, proper characterization and control experiments will be needed when applying the probes in ascorbate quantification in real samples.

**Table 1.** Ascorbate analysis using AP-cyan on drinks, human plasma and serum samples.

Samples	ascorbate concentration		
	diluted sample <sup>[a]</sup>	original sample	reported
Nice 100% Apple Juice	6.81±0.07 M	1.36±0.01 mM	1.70 mM <sup>[b]</sup>
Glacéau Vitamin Water Power-C	6.63±0.19 M	1.32±0.04 mM	1.31 mM <sup>[c]</sup>
Plasma	0.24±0.04 M	48±8 M	46.5 M <sup>[30]</sup>
Serum	0.32±0.03 M	64±6 M	51.4 M <sup>[31]</sup>

[a]: n = 3; dilution factor = 200; [b]: value given in the food label = 0.30 mg/mL; [c]: value given in the food label = 0.23 mg/mL

**Fluorescent Imaging of Ascorbate Uptake in Live Cells.** As previously discussed, current strategies for ascorbic acid detection are limited for use in living systems. Due to the stability, selectivity, and sensitivity of AP-cyan, we were interested in evaluating its performance in live cells. Prior to performing live-cell imaging, we assessed the biocompatibility of AP-cyan where no significant cytotoxicity was observed under typical imaging conditions (Figure S27). In particular, a cellular ascorbate uptake model was selected because the vitamin cannot be synthesized in human cells. Although ascorbate uptake pathways are cell type dependent and poorly characterized, transport of DHA via glucose transporters (e.g. GLUT1 or GLUT3) has been proposed due to the structural similarity of the sugar and DHA.<sup>[32]</sup> Following cell uptake, one would expect that DHA would be reduced to ascorbate upon entering the reducing environment of the cell. Previous studies have employed radioisotope labelling and HPLC to study DHA transport.<sup>[33]</sup> While successful, these methods may be technically challenging and have no specificity on ascorbate redox state. Fluorescence imaging is an attractive alternative to radiolabeled approaches because it allows direct visualization of ascorbate within cells. Moreover, the fluorescence enhancement reports on the activity of the ascorbate rather than strictly the concentration, which should more closely parallel the biological effects.<sup>[34]</sup>

First, HeLa cells were stained with AP-cyan and then treated with media enriched with variable concentrations DHA (0, 0.5, and 1.0 mM) for 15 min. Under these conditions, we observed a dose-dependent response to DHA (Figure 3). Motivated by these results, we were interested in confirming whether GLUT1 and GLUT3 are responsible for DHA uptake. To address this question, HeLa cells were stained with AP-cyan followed by incubation with 1 mM DHA supplemented media either in the presence of 10 mM D-glucose or D-fructose. Co-incubation of 1 mM DHA and 10 mM D-glucose decreased the fluorescence by 41%, presumably via competitive inhibition at the glucose transporters.<sup>[31c]</sup> D-fructose, which is not a ligand for glucose transporters, had less of an effect on the observed fluorescence (Figure 3). These experiments establish AP-cyan as a suitable tool for imaging ascorbate in live cells and provides additional experimental evidence for ascorbate trafficking via GLUT uptake of DHA followed by intracellular reduction.

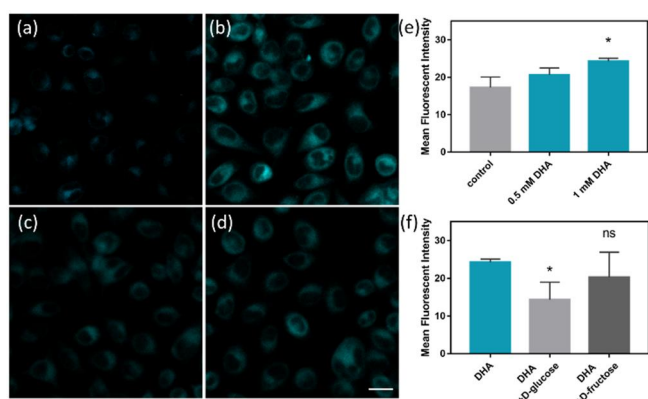


**Figure 3.** Confocal microscopy images of HeLa cells treated with AP-cyan (50  $\mu$ M, 15 min) then (a) 0 mM DHA (vehicle control); (b) 1 mM DHA; (c) 1 mM DHA with 10 mM D-glucose; or (d) 1 mM DHA with 10 mM D-fructose for 15 min at 37°C. Quantification of (e) DHA concentrations and (f) GLUT transporter inhibition studies. The probe was excited at 488 nm and emission was collected between 493 nm–735 nm. Scale bar represents 20  $\mu$ m. Mean fluorescence is reported as the mean of biological replicated  $\pm$  standard deviation. Statistical analysis was performed using two-tailed Student's *t*-test: \*:  $p < 0.05$  ( $n = 3$ ).

**Application of AP-green in Flow Cytometry.** Finally, intracellular detection of ascorbate was performed using flow cytometry. Flow cytometric analyses are complementary to confocal microscopy because they enable rapid detection of large cell populations but lack spatial resolution. AP-green ( $\lambda_{\text{ex}} = 488$  nm,  $\lambda_{\text{em}} = 510$  nm) was selected for these experiments due to good spectral overlap with the ubiquitous FITC excitation source. A large shift in fluorescence was observed for HeLa cells that were cultured in a DHA-enriched media as compared to the untreated control (Figure S28). Importantly, this experiment demonstrates the advantage of the bond cleavage detection strategy where the modular trigger allows for facile tuning of the photophysical properties of the probe. More generally, one could envision the modular optimization of other properties (e.g. analytical or biological) due to the uncapping approach.

## Conclusion

In summary, a novel bond cleavage strategy was reported for the activity-based sensing of ascorbate. Contrary to the reducing nature of ascorbate, a copper-mediated oxidative ether bond cleavage is exploited for the release of a covalently caged fluorescent reporter. AP-cyan and AP-green display good sensitivity and selectivity and maintain their functionality in complex matrices (e.g. commercial food samples, human plasma, serum and live cells). By utilizing a fluorescent readout, both probes are compatible with plate reader fluorimeters, confocal microscopy and flow cytometry for high throughput quantification, high resolution detection and detection in large cell populations. In addition, the ascorbate responsive unit can be modularly attached to different fluorophores without affecting

the reactivity and selectivity, providing a versatile strategy for tuning a variety of properties. Finally, the selective metal-mediated bond cleavage could be a versatile strategy for developing other analyte-responsive sensors. This would represent a new direction in activity-based sensing that relies on complementarity chemical reactivity between multiple species.

## Acknowledgements

This work was supported by the Croucher Foundation and the Research Grants Council of the Hong Kong Special Administrative Region, China (HKU 106150183). Z. H. Y. is a recipient of the Postgraduate Scholarship from The University of Hong Kong. C.J.R. thanks the Chemistry-Biology Interface Training Grant (T32GM070421). We thank Dr. C. N. Lok, Dr. A. Y. Z. Lai and Dr. Y. Yang for their assistance in initial experiments and Prof. Jefferson Chan for his helpful support on this project. We acknowledge UGC funding administered by The University of Hong Kong for supporting the Electrospray Ionization Quadrupole Time-of-Flight Mass Spectrometry Facilities under the Support for Interdisciplinary Research in Chemical Science. We also acknowledge the Core Facilities at the Carl R. Woese Institute for Genomic Biology for access to the Zeiss LSM 700 Confocal Microscope and corresponding software. We acknowledge support from the HKU Li Ka Shing Faculty of Medicine Imaging and Flow Cytometry Core for access to the BD LSR Fortessa Analyzer.

**Keywords:** activity-based sensing ~ ascorbate ~ copper ~ fluorescent probe ~ oxidation

- [1] (a) J. Du, J. J. Cullen, G. R. Buettner, *Biochim. Biophys. Acta* **2012**, *1826*, 443; (b) N. Smirnov, G. L. Wheeler, *Crit. Rev. Bio. Mol. Biol.* **2000**, *35*, 291; (c) J. L. Svrbely, A. Szent-Györgyi, *Biochem. J* **1933**, *27*, 279.
- [2] (a) M. B. Davies, D. A. Partridge, J. A. Austin in *Vitamin C: Its Chemistry and Biochemistry*, Royal Society of Chemistry, **1991**; (b) C. Creutz, *Inorg. Chem.* **1981**, *20*, 4449.
- [3] C. H. Foyer, G. Noctor, *Plant Physiol.* **2011**, *155*, 2.
- [4] (a) B. H. J. Bielski, A. O. Allen, H. A. Schwarz, *J. Am. Chem. Soc* **1981**, *103*, 3516; (b) G. R. Buettner, *Arch. Biochem. Biophys* **1993**, *300*, 535; (c) A. Jimenez, J. A. Hernandez, L. A. del Rio, F. Sevilla, *Plant Physiol.* **1997**, *114*, 275. (d) O. Arrigoni, M. C. De Tullio, *Biochim. Biophys. Acta* **2002**, *1569*, 1.
- [5] S. Murad, D. Grove, K. A. Lindberg, G. Reynolds, A. Sivarajah, S. R. Pinnell, *Proc. Natl. Acad. Sci. USA* **1981**, *78*, 2879.
- [6] J. D. Hulse, S. R. Ellis, L. Henderson, *J. Biol. Chem.* **1978**, *253*, 1654.
- [7] A. G. Katopodis, S. W. May, *Biochemistry* **1990**, *29*, 4541.
- [8] F. Menniti, J. Knoth, E. Diliberto, *J. Biol. Chem.* **1986**, *261*, 16901.
- [9] K. A. Naidu, *Nutr. J.* **2003**, *2*, 7.
- [10] Z. Gazdik, O. Zitka, J. Petrova, V. Adam, J. Zehnalek, A. Horna, V. Reznicek, M. Beklova, R. Kizek, *Sensors* **2008**, *8*, 7097.
- [11] V. Arabali, M. Ebrahimi, M. Abbasghorbani, V. K. Gupta, M. Farsi, M. Ganjali, F. Karimi, *J. Mol. Liq.* **2016**, *213*, 312.
- [12] C. K. M. Choy, I. F. F. Benzie, P. Cho, *Invest. Ophth. Vis. Sci.* **2000**, *41*, 3293.
- [13] (a) C. Li, A. G. Tebo, A. Gautier, *Int. J. Mol. Sci.* **2017**, *18*, E1473; (b) E. A. Specht, E. Braselmann, A. E. Palmer, *Annu. Rev. Physiol.* **2017**, *79*, 93.
- [14] (a) K. Ishii, K. Kubo, T. Sakurada, K. Komori, Y. Sakai, *Chem. Commun.* **2011**, *47*, 4932; (b) B. Song, Z. Ye, Y. Yang, H. Ma, X. Zheng, D. Jin, J.



- Yuan, *Sci. Rep.* **2015**, *5*, 14194; (c) C.-P. Liu, T.-H. Wu, C.-Y. Liu, H.-J. Cheng, S.-Y. Lin, *J. Mater. Chem. B* **2015**, *3*, 191; (d) W. Zhai, C. Wang, P. Yu, Y. Wang, L. Mao, *Anal. Chem.* **2014**, *866*, 12206; (e) P. Zhao, K. He, Y. Han, Z. Zhang, M. Yu, H. Wang, Y. Huang, Z. Nie, S. Yao, *Anal. Chem.* **2015**, *87*, 9998.
- [15] (a) G. Vaaje-Kolstad, B. Westereng, S. J. Horn, Z. Liu, H. Zhai, M. Sørlie, V. G. H. Eijsink, *Science* **2010**, *330*, 219; (b) R. J. Quinlan, M. D. Sweeney, L. L. Leggio, H. Otten, J.-C. N. Poulsen, K. S. Johansen, K. B. R. M. Krogh, C. I. Jørgensen, M. Tovborg, A. Anthonsen, T. Tryfona, C. P. Walter, P. Dupree, F. Xu, G. J. Davies, P. H. Walton, *Proc. Natl. Acad. Sci. USA* **2011**, *108*, 15079; (c) C. M. Phillips, W. T. Beeson IV, J. H. Cate, M. A. Marletta, *ACS Chem. Biol.* **2011**, *6*, 1399; (d) Z. Forsberg, G. Vaaje-Kolstad, B. Westereng, A. C. Bunæs, Y. Stenstrøm, A. MacKenzie, M. Sørlie, S. J. Horn, V. G. H. Eijsink, *Protein Sci.* **2011**, *20*, 1479; (e) A. Levasseur, E. Drula, V. Lombard, P. M. Coutinho, B. Henrissat, *Biotechnol. Biofuels* **2013**, *6*, 41; (f) G. R. Hemsworth, B. Henrissat, G. J. Davies, P. H. Walton, *Nat. Chem. Biol.* **2014**, *10*, 122; (g) L. Ciano, G. J. Davies, W. B. Tolman, P. H. Walton, *Nature Catalysis* **2018**, *1*, 571.
- [16] (a) K. E. H. Frandsen, T. J. Simmons, P. Dupree, J.-C. N. Poulsen, G. R. Hemsworth, L. Ciano, E. M. Johnston, M. Tovborg, K. S. Johansen, P. von Freiesleben, L. Marmuse, S. Fort, S. Cottaz, H. Driguez, B. Henrissat, N. Lenfant, F. Tuna, A. Baldansuren, G. J. Davies, L. L. Leggio, Paul. H. Walton, *Nat. Chem. Biol.* **2016**, *12*, 298; (b) S. Karkehabadi, H. Hansson, S. Kim, K. Piens, C. Mitchinson, M. Sandgren, *J. Mol. Biol.* **2008**, *383*, 144; (c) X. Li, W. T. Beeson IV, C. M. Phillips, M. A. Marletta, J. H. D. Cate, *Structure* **2012**, *20*, 1051.
- [17] (a) D. Kracher, S. Scheiblbrandner, A. K. G. Felice, E. Breslmayr, M. Preims, K. Ludwicka, D. Haltrich, V. G. H. Eijsink, R. Ludwig, *Science* **2016**, *352*, 1098; (b) M. Frommhagen, M. J. Koetsier, A. H. Westphal, J. Visser, S. W. A. Hinz, J.-P. Vincken, W. J. H. van Berkel, M. A. Kabel, H. Gruppen, *Biotechnol. Biofuels* **2016**, *9*, 186; (d) P. H. Walton, G. J. Davies, *Curr. Opin. Chem. Biol.* **2016**, *31*, 195.
- [18] (a) M. Taki, S. Iyoshi, A. Ojida, I. Hamachi, Y. Yamamoto, *J. Am. Chem. Soc.* **2010**, *132*, 5938; (b) H.Y. Au-Yeung, E.J. New, C.J. Chang, *Chem. Commun.* **2012**, *48*, 5268; (c) H.Y. Au-Yeung, J. Chan, T. Chantarojsiri, C.J. Chang, *J. Am. Chem. Soc.* **2013**, *135*, 15165.
- [19] (a) Y. Hitomi, T. Takeyasu, T. Funabiki, M. Kodera, *Anal. Chem.* **2011**, *83*, 9213; (b) Y. Hitomi, T. Takeyasu, M. Kodera, *Chem. Commun.* **2013**, *49*, 9929; (c) Z. H. Yu, C. Y.-S. Chung, F. K. Tang, T. F. Brewer, H. Y. Au-Yeung, *Chem. Commun.* **2017**, *53*, 10042; (d) K. Y. Tong, J. Zhao, C.-W. Tse, P.-K. Wan, J. Rong, H. Y. Au-Yeung, *Chem. Sci.* **2019**, *10*, 8519; (e) F. K. Tang, Z. H. Yu, T. H.-F. Wong, C. Y.-S. Chung, H. Hirao, H. Y. Au-Yeung, *ChemPlusChem* **2020**, *85*, 653.
- [20] (a) S. Ando, K. Koide, *J. Am. Chem. Soc.* **2012**, *134*, 17486; (b) W. Lin, L. Long and W. Tan, *Chem. Commun.* **2010**, *46*, 1503; (c) Y. Zhao, Q. Zheng, K. Dakin, K. Xu, M. L. Martinez, W.-H. Li, *J. Am. Chem. Soc.* **2004**, *126*, 4653.
- [21] H. Y. Au-Yeung, C. Y. Chan, K. Y. Tong, Z. H. Yu, *J. Inorg. Biochem.* **2017**, *177*, 300.
- [22] (a) M. M. Olmstead, T. E. Patten, C. Troeltzsch, *Inorg. Chim. Acta* **2004**, *357*, 619; (b) J. W. Shin, A. R. Jeong, S. Y. Lee, C. Kim, S. Hayami, K. S. Min, *Dalton Trans.* **2016**, *45*, 14089.
- [23] O. S. Wolfbeis, E. Koller, P. Hochmuth, *Bull. Chem. Soc. Jpn.* **1985**, *58*, 731.
- [24] (a) S. I. Mann, T. Heinisch, T. R. Ward, A. S. Borovik, *J. Am. Chem. Soc.* **2017**, *139*, 17289; (b) A. L. Concia, M. R. Beccia, M. Orio, F. T. Ferre, M. Scarpellini, F. Biaso, B. Guigliarelli, M. Réglie, A. J. Simaan, *Inorg. Chem.* **2017**, *56*, 1023; (c) A. C. Neira, P. R. Martínez-Alanis, G. Aullon, M. Flores-Alamo, P. Zeron, A. Company, J. Chen, J. B. Kasper, W. R. Browne, E. Nordlander, I. Castillo, *ACS Omega* **2019**, *4*, 10729.
- [25] As aqueous solubility AP-green and AP-cyan is not high enough for CV studies, the model complex [Cu(7)Cl<sub>2</sub>] was used.
- [26] One-electron reduction potential of ascorbate has been determined to be +0.33 V vs. NHE, see: D. Njus, P. M. Kelley, *FEBS Lett.* **1991**, *284*, 147.
- [27] (a) J. J. Warren, J. M. Mayer, *J. Am. Chem. Soc.* **2010**, *132*, 7784; (b) V. Cuculi, M. Mlakar, M. Branica, *Electroanal.* **1998**, *10*, 852.
- [28] J. Xu, R. B. Jordan, *Inorg. Chem.* **1990**, *29*, 2933.
- [29] (a) M. H. Zweig, A. Jackson, *Clin. Chem.* **1986**, *32*, 674; (b) G. Ceglie, G. Macchiarulo, M. R. Marchili, A. Marchesi, L. Rotondi Aufiero, C. Di Camillo, A. Villani, *Arch. Dis. Child.* **2019**, *104*, 381.
- [30] W. Y. Chung, J. K. O. Chung, Y. T. Szeto, B. Tomlinson, I. F. Benzie, *Clin. Biochem.* **2001**, *34*, 623
- [31] R. L. Schleicher, M. D. Carroll, E. S. Ford, D. A. Lacher, *Am. J. Clin. Nutr.* **2009**, *90*, 1252.
- [32] (a) J. X. Wilson, *Annu. Rev. Nutr.* **2005**, *25*, 105; (b) R. L. Ingermann, L. Stankova, R. H. Bigley, *Am. J. Physiol. Cell. Physiol.* **1986**, *250*, C637; (c) S. C. Rumsey, O. Kwon, G. W. Xu, C. F. Burant, I. Simpson, M. Levine, *J. Biol. Chem.* **1997**, *272*, 18982.
- [33] J. C. Vera, C. I. Rivas, J. Fischberg, D. W. Golde, *Nature* **1993**, *364*, 79.
- [34] J. Chan, S. C. Dodani, C. J. Chang, *Nat. Chem.* **2012**, *4*, 973.

## Entry for the Table of Contents



A new activity-based sensing strategy was developed for the highly selective detection of ascorbate. A copper(II) complex was designed to be activated by ascorbate to effect an oxidative bond cleavage and release an emissive fluorophore for a turn-on signal. The new ascorbate probes can be applied in complex matrix including food, plasma and live cells.

Institute and/or researcher Twitter usernames: @hku\_science @HYAGroup @ChanLabUIUC